Langmuir

Article

pubs.acs.org/Langmuir

Wet Chemical Functionalization of III−V Semiconductor Surfaces: Alkylation of Gallium Arsenide and Gallium Nitride by a Grignard Reaction Sequence

Sabrina L. Peczonczyk,[†] Jhindan Mukherjee,[†] Azhar I. Carim,[†] and Stephen Maldonado*[,†,‡]

[†]Department of Chemistry and [‡]Program in Applied Physics, University of Michigan, 930 North University Avenue, Ann Arbor, Michigan 48109-1055, United States

Supporting Information

ABSTRACT: Crystalline gallium arsenide (GaAs) (111)A and gallium nitride (GaN) (0001) surfaces have been functionalized with alkyl groups via a sequential wet chemical chlorine activation, Grignard reaction process. For GaAs(111)A, etching in HCl in diethyl ether effected both oxide removal and surface-bound Cl. X-ray photoelectron (XP) spectra demonstrated selective surface chlorination after exposure to 2 M HCl in diethyl ether for freshly etched GaAs(111)A but not GaAs(111)B surfaces. GaN(0001) surfaces exposed to PCl_5 in chlorobenzene showed reproducible XP spectroscopic evidence for Cl-termination. The Cl-activated GaAs(111)A and GaN(0001) surfaces were both reactive toward alkyl Grignard reagents, with pronounced decreases in detectable Cl signal as measured by XP spectroscopy. Sessile contact angle measurements between water and GaAs(111)A interfaces after various levels of treatment showed that GaAs(111)A surfaces became significantly more hydrophobic following reaction with $C_nH_{2n-1}MgCl$ (n = 1, 2, 4, 8, 14, 18). High-resolution As 3d XP spectra taken at various times during prolonged direct exposure to ambient lab air indicated that the resistance of GaAs(111)A to surface oxidation was greatly enhanced after reaction with Grignard reagents. GaAs(111)A surfaces terminated with $C_{18}H_{37}$ groups were also used in Schottky heterojunctions with Hg. These heterojunctions exhibited better stability over repeated cycling than heterojunctions based on GaAs(111)A modified with $C_{18}H_{37}S$ groups. Raman spectra were separately collected that suggested electronic passivation by surficial Ga−C bonds at GaAs(111)A. Specifically, GaAs(111)A surfaces reacted with alkyl Grignard reagents exhibited Raman signatures comparable to those of samples treated with 10% Na_2S in *tert*-butanol. For GaN(0001), high-resolution C 1s spectra exhibited the characteristic low binding energy shoulder demonstrative of surface Ga−C bonds following reaction with CH_3MgCl. In addition, 4-fluorophenyl groups were attached and detected after reaction with C_6H_4FMgBr, further confirming the susceptibility of Cl-terminated GaN(0001) to surface alkylation. However, the measured hydrophobicities of alkyl-terminated GaAs(111)A and GaN(0001) were markedly distinct, indicating differences in the resultant surface layers. The results presented here, in conjunction with previous studies on GaP, show that atop Ga atoms at these crystallographically related surfaces can be deliberately functionalized and protected through Ga−C surface bonds that do not involve thiol/sulfide chemistry or gas-phase pretreatments.

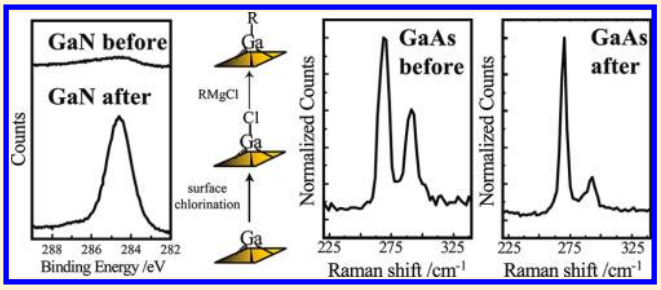

INTRODUCTION

Gallium-based III−V semiconductors such as GaAs and GaN are the key materials in many existing and emerging optoelectronic technologies for chemical sensing, lighting, and solar energy conversion. One common drawback to these materials is that the quality of their native surfaces is easily compromised under ambient conditions. Relative to the vast wet chemical reaction sequences available for group IV semiconductor surfaces,[1−8] there are comparatively few established wet chemical methodologies for modifying the native surfaces of GaAs and GaN.[9−14] The most effective and most common type of wet chemical reactions for functionalizing GaAs and GaN surfaces involves immersion in solutions with sulfur-containing reagents (e.g., Na_2S or alkanethiols),[15−23] affecting the observable wetting properties, the surface energetics (i.e., the conduction and valence band edge electrochemical potentials), and/or surface charge trap density.[24−28] Although a comprehensive analysis of thiol/sulfide treatments is outside the scope of this report, the main conclusions to be drawn from decades of research are that these wet chemical strategies were not designed from a detailed molecular-level understanding of surface reactivity and are accordingly not adequate in many optoelectronic applications. For example, thiol-based treatments are inferior to epitaxial surface capping layers (e.g., $Al_xGa_{1-x}As$, SiN_x)[29−33] for ameliorating surface defects long-term. To determine whether any wet chemical strategy for III−V surfaces can supplant costly and complex solid-state surface treatments, better insight on the wet chemical reactivity of these semiconductor interfaces is needed.

For GaAs, the (111) surface plane features atop surface atoms with three bonding orbitals involved in bulk lattice

Received: November 28, 2011
Revised: February 8, 2012
Published: February 28, 2012

   dx.doi.org/10.1021/la204698a | Langmuir 2012, 28, 4672−4682

bonding and one available bonding orbital directed normal to the surface. Unreconstructed GaAs(111) surfaces that feature only partially coordinated Ga atop atoms are denoted as GaAs(111)A (Figure 1a). Similarly, crystalline wurtzite GaN ideally features only partially coordinated atop Ga atoms on the (0001) surface plane (Figure 1a). Provided that nonoxidized, chemically uniform GaAs(111)A and GaN(0001) surfaces can first be prepared through etching/cleaning treatments, the chemical reactivity of these two surface planes should largely reflect the reactivity of the atop Ga atoms.

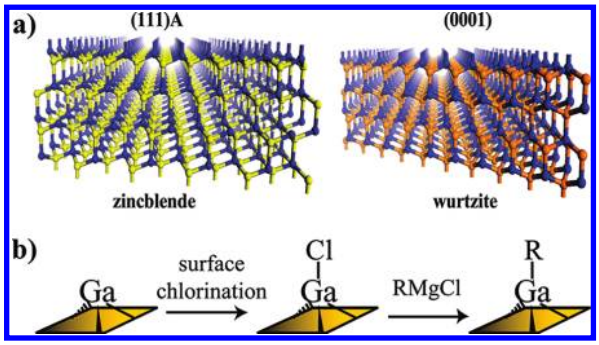

Figure 1. (a) Graphical representation of (left) zincblende GaAs and (right) wurtzite GaN crystal slabs. The (111)A and (0001) faces are at the top of each slab, respectively, and feature an atop Ga atom with one bonding orbital not participating in lattice bonding. (b)Wet chemical functionalization of atop Ga atoms at GaAs(111)A and GaN(0001) surfaces through surface Ga−C bonds produced through sequential chlorination and reaction with a Grignard reagent.

Our group has recently demonstrated that alkyl chains can be covalently grafted onto single-crystalline GaP(111)A surfaces via a two-step chlorination/alkylation reaction sequence using Grignard reagents.[34] The resultant GaP surfaces were resistant to surface oxidation, consistent with the presence of a protective organic group bound through a Ga−C covalent linkage. Herein, we present data that explore this reaction sequence applied to GaAs(111)A and GaN(0001) surfaces. The primary hypotheses of this work are that atop Ga atoms at these interfaces are selectively reactive toward nucleophilic alkylation reagents and that this surface bonding motif can address some of the deficiencies of native GaAs and GaN interfaces. Specifically, we have collected data that explore the viability of Grignard reagents (Figure 1b) for modifying GaAs(111)A and GaN(0001) interfaces. We present a series of spectroscopic and electrical data that collectively describe chemically modified GaAs and GaN surfaces, highlighting this wet chemical strategy for controlling the properties of these semiconductor interfaces.

EXPERIMENTAL SECTION

Materials and Chemicals. Unless noted otherwise, chemicals were from Aldrich. Methanol (low water content, JT Baker), ethanol (95%, Fisher), acetone (HPLC-grade, Fisher), tetrahydrofuran (anhydrous, Acros), CH_3MgCl (3.0 M solution in THF), C_2H_5MgCl (2.0 M solution in THF), C_4H_7MgCl (2.0 M solution in THF), $C_8H_{17}MgCl$ (2.0 M solution in THF), $C_{14}H_{29}MgCl$ (1.0 M solution in THF), $C_{18}H_{37}MgCl$ (0.5 M solution in THF), C_6H_4FMgBr (1.0 M in THF), $C_{18}H_{37}SH$ (98%), HCl (2.0 M solution in diethyl ether), HCl, NH_4OH (30% NH_3 in H_2O), PCl_5 (95%), chlorobenzene (anhydrous 99.8%), doubly distilled H_2SO_4 (95−98%, *tert*-butyl alcohol (99%), Na_2S (90%), and KOH (85%, Acros) were used as received. Benzoyl peroxide (≥97%) was purchased from Fluka and dried under a vacuum of <200 mTorr for 24 h. Water with a resistivity >18 MΩ·cm (Barnsted Nanopure system) was used throughout. GaAs(111) wafers (ITME) doped with Zn at 3.1×10^{17} cm^{-3} with a thickness of 400 ± 20 μm were used for reaction and physicochemical characterization. GaAs(111) wafers (ITME) doped with Si at 2.6×10^{16} cm^{-3} with a thickness of 500 ± 25 μm were used for electrical measurements. GaAs(111) wafers (ITME) doped with Te at 1.1×10^{18} cm^{-3} with a thickness of 385 ± 25 μm were used for Raman measurements. Undoped *n*-GaN(0001) films on c-plane sapphire (5 μm ± 2 μm) were either obtained through chemical vapor deposition with $Ga(CH_3)_3$ and NH_3 or purchased from Kyma Technologies.

Etching. Prior to use, samples were cut into square ∼0.5 cm^2 sections and degreased by sequential rinsing in water, methanol, acetone, methanol and water. To remove native oxides, GaAs(111) samples were etched in concentrated H_2SO_4(aq) for 30 s, while GaN(0001) samples were etched in 1 M KOH(aq) at 70 °C for 2 min. Etched samples were rinsed with copious amounts of water and dried with a stream of N_2(g) before further use.

Chlorine Activation and Grignard Reaction. All reactions were performed in an MBraun LABstar glovebox purged and pressurized with dry N_2(g). The residual O_2 and H_2O content in the glovebox were assessed by use of diethyl zinc and an exposed tungsten filament.[35,36] An open container of diethyl zinc in the glovebox did not combust or substantially fume. Separately, an exposed tungsten filament remained lit for >7 min, indicating that H_2O and O_2 levels were at 100 ppm or lower after purging with N_2(g). Chlorination of GaN(0001) was performed at 95 °C for 50 min in a saturated solution of PCl_5 in chlorobenzene containing a few grains of benzoyl peroxide.[34,37] This treatment macroscopically roughened both GaAs(111) surface planes. Attempts were made to perform this reaction at lower temperatures and for shorter time periods, but PCl_5 in chlorobenzene effected bulk etching of GaAs under all investigated reaction conditions. Accordingly, GaAs(111)A surfaces were immersed in a 2 M solution of HCl in diethyl ether for 50 min. The sample was then rinsed with anhydrous tetrahydrofuran (THF). For samples used for further functionalization, the substrates were directly reacted with the next reagent without exposure to ambient. For X-ray photoelectron (XP) analysis, Cl-activated surfaces were exposed briefly (<15 s) to ambient before insertion into the X-ray photoelectron spectrometer.

Reactions with Grignard reagents were performed at 145−150 °C for 3 h in a closed, pressurized thick glass vessel. These vessels were heated with a solid heating block. Following, samples were rinsed sequentially with anhydrous THF and anhydrous methanol. Samples were subject to an additional sonication step in a protic solvent for 2 min to remove any physisorbed Cl- and Mg-containing species.

X-ray Photoelectron Spectroscopy. All X-ray photoelectron spectra were acquired with a PHI 5400 analyzer using an Al Kα (1486.6 eV) source without a monochromator. Spectra were recorded without charge neutralization at a base pressure of $<2.5 \times 10^{-9}$ Torr. A 6 mA emission current and 10 kV anode HT was used. Survey scans were acquired at a pass energy of 117.40 eV. High-resolution XP spectra of Ga 3d, As 3d, C 1s, and Cl 2p regions were recorded at a pass energy of 23.5 eV. The binding energy of all spectra were corrected by use of the difference between the observed peak energy of the C 1s signal and the expected binding energy for adventitious carbon at 284.6 eV.[38] Average times for acquiring high-resolution spectra (100 scans) for each element ranged from 30 to 45 min. Samples did not undergo any observable degradation upon exposure to the X-ray source under these conditions.

Spectra were fitted and analyzed by use of CasaXPS version 2.313 software. A Shirley background correction was applied to all spectra. As 3d peaks were fit with a 70% Gaussian and 30% Lorentzian line shape, a pair of doublets that were mutually constrained to have an area ratio of 3:2, and the same full width at half maximum (ranging from 0.9 to 1.2), and peak separation of 0.69 eV.[39,40] Fractional monolayer coverage of oxidized GaAs surfaces were calculated from the simplified substrate overlayer model:[40]

$$d = \lambda_{ov} \ln\left(1 + \frac{I_{overlayer}}{I_{substrate}} \frac{I^0_{substrate}}{I^0_{overlayer}}\right) \sin\phi \quad (1)$$

dx.doi.org/10.1021/la204698a | *Langmuir* 2012, 28, 4672−4682

where d is the thickness of the oxide overlayer in nanometers, λ_{ov} is the escape depth of the emitted electrons through the oxide overlayer, ϕ is the takeoff angle (54.6°), $I_{substrate}$ is the integrated area of As 3d signal from the bulk crystal, $I_{overlayer}$ is the integrated area of the oxide As 3d signals, $I^0_{substrate}$ is the integrated intensity of As 3d signals obtained from a GaAs surface etched with H_2SO_4 (aq) for 30 s, and $I^0_{overlayer}$ is the integrated intensity of the As 3d oxide signatures from a pure oxide of GaAs. To determine this value, thick thermal oxides were not tenable,[41,42] so $I^0_{overlayer}$ was estimated with a heavily chemically oxidized substrate. The escape depths of As 3d electrons were estimated from eq 2:

$$\lambda = 0.41\alpha^{3/2}E^{1/2} \tag{2}$$

where α is the diameter of the atoms in the overlayer in nanometers and E is the kinetic energy of the ejected core electron in electronvolts.[40] The escape depth was 2.1 nm for As 3d electrons. The surface coverage of Cl-terminated GaAs(111)A and GaN(0001) was calculated from the full substrate overlayer model:[40]

$$\left(\frac{I_{ov}}{I_{Ga}}\right) = \left(\frac{SF_{ov}}{SF_{sub}}\right)\left(\frac{\rho_{ov}}{\rho_{sub}}\right)\left(\frac{1 - e^{-d_{ov}/\lambda_{ov}\sin\phi}}{e^{-d_{ov}/\lambda_{sub}\sin\phi}}\right) \tag{3}$$

where SF_{sub} is the instrument sensitivity factor for the element of interest in the substrate, SF_{ov} is the instrument sensitivity factor for the element of study in the overlayer, ρ_{sub} is the molar density of the element of interest in the substrate (moles per cubic centimeter), ρ_{ov} is the density of the element of interest in the overlayer (moles per cubic centimeter), and the other symbols are as defined above.

For time-dependent oxide growth measurements, surface-modified samples were first introduced into the XPS load-lock chamber immediately following functionalization. Subsequent measurements were taken by exposure of the sample to laboratory ambient for a designated period of time in the spectrometer load-lock chamber and then reinsertion back into the XPS chamber. For water studies, samples were immersed in water, removed and dried under flowing N_2(g), and then reintroduced into the XPS load-lock.

Static Sessile Drop Contact Angle Measurements. A water droplet (~2.2 μL) was dispensed onto the surface of each interrogated sample. Each contact angle formed between the droplet and sample interface was recorded with a CAM 100 optical contact angle meter (KSV Instrument, Helsinki, Finland). Images of the droplets were acquired and analyzed by use of the KSV software analysis package. The reported values are the average equilibrium contact angles (θ_0), which were calculated from the advancing contact angle (θ_A) and receding contact angle (θ_R).[43,44] The uncertainties in θ_0 are reported as sample standard deviations.

$$\theta_0 = \arccos\left[\left(\sqrt[3]{\frac{\sin^3\theta_A}{2 - 3\cos\theta_A + \cos^3\theta_A}}\cos\theta_A + \sqrt[3]{\frac{\sin^3\theta_R}{2 - 3\cos\theta_R + \cos^3\theta_R}}\cos\theta_R\right) \Big/ \left(\sqrt[3]{\frac{\sin^3\theta_A}{2 - 3\cos\theta_A + \cos^3\theta_A}} + \sqrt[3]{\frac{\sin^3\theta_R}{2 - 3\cos\theta_R + \cos^3\theta_R}}\right)\right] \tag{4}$$

Raman Spectroscopy. Raman spectra were acquired with a Renishaw inVia spectrometer arranged in a 180° backscatter geometry and equipped with a Leica microscope, Leica 100× N Plan EPI objective (NA = 0.85), dielectric edge filter, 1800 lines/mm grating, and a charge-coupled device (CCD) detector. The 457.9 nm line of a Ar^+ laser (Coherent Innova 307) was used as the excitation with a radiant power of 160 μW incident on the sample. Optical excitation was directed along the ⟨111⟩ direction and polarized along the ⟨11$\bar{0}$⟩ direction. No polarization optics were used for the detection of scattered light. This excitation is strongly absorbed by GaAs ($\alpha_{GaAs,458nm}$ = 1.9 × 10^5 cm^{-1}),[45] that is, the Raman scatter arises from the near surface region. The use of an objective with a high numerical aperture also ensured that the collection of scattered light was predominantly from the near surface region. Hence, these spectral acquisition conditions were chosen specifically to collect Raman spectra that reported on the surface to near-surface regions of heavily doped GaAs samples. Unfortunately, an appropriate excitation wavelength for GaN that would similarly effect surface-sensitive Raman signals was not available, and so no attempt was made to acquire Raman spectra for GaN. Integrated areas of the Γ(TO) and Γ(LO) modes were determined through fitting spectra with Wire 3.1 software. The best fits were obtained for each signature by use of a line shape composed of 55% Gaussian and 45% Lorentzian character. For comparison, GaAs(111)A samples were also treated by immersion in a 10% (v/v) Na_2S solution in *tert*-butanol for 6–8 h in a N_2(g) purged glovebox and then analyzed under ambient conditions.[46−48]

Hg/GaAs Heterojunctions. Several methods for preparing ohmic back contacts were explored. Initial efforts followed the procedure of Nesher et al.[25] First, the backside was gently scratched with a diamond scribe and then immediately coated with a thin layer of InGa eutectic. Spot contacts separated by 2–3 mm showed a total resistance of 100–120 Ω but the current–potential responses between these spot contacts were decidedly nonlinear; that is, these contacts did not exhibit ideal ohmic behavior. Therefore, an alternative contacting strategy was used.[34] Briefly, the backside was scratched, etched in H_2SO_4(aq), and then coated with a thin layer of In solder. The sample was purged in a tube furnace with Ar for 50 min at a flow rate of 1000 $cm^3{\cdot}min^{-1}$, annealed at 400 °C for 10 min in a stream of Ar(g) and forming gas [5:95 v/v H_2(g)/N_2(g)] at a flow rate of 50 $cm^3{\cdot}min^{-1}$, and slowly cooled to room temperature in Ar(g). For functionalization, only the nonsoldered part of the crystal was exposed to reagents so that the ohmic contact remained uncompromised. For functionalization with $C_{18}H_{37}S$ moieties, the nonsoldered part of sample was etched and immediately immersed for 24 h in a freshly prepared ethanolic solution of 0.003 M $C_{18}H_{37}SH$ and 0.01 M NH_4OH.[20] The solution was deaerated and degassed in dry N_2(g) prior to use. After surface passivation, the wafer was thoroughly rinsed in ethanol and immediately used for further studies. A Hg droplet was placed on the front surface of a GaAs wafer section resting on a stainless steel support that acted as the back contact. A Viton O-ring was used to define the junction area (0.063 cm^2) between GaAs and the Hg droplet. A Pt wire was used to make electrical contact to the Hg droplet. Current–voltage responses were measured in the dark, with a CH Instruments 420a potentiostat at a scan rate of 0.05 $V{\cdot}s^{-1}$.

RESULTS

GaAs. Unlike our earlier report on Cl-termination of GaP(111)A interfaces,[34] wet chemical chlorination of GaAs(111)A surfaces through immersion in dissolved PCl_5 in chlorobenzene consistently effected severe etching/pitting. Aqueous HCl(aq) has previously been used to introduce surficial Cl at GaAs(111)A.[39] To avoid the possibility of residual Ga surface hydroxides from an aqueous chlorination step,[39,49] HCl in diethyl ether facilitated surface chlorination in a controlled environment in a N_2(g) glovebox. Figure 2a shows high-resolution XP spectra highlighting the Cl 2p doublet near the As 3s signal. Selective chlorination of GaAs(111)A over GaAs(111)B surfaces was observed, with no detectable level of Cl at GaAs(111)B surfaces. The Cl signatures in Figure 2a could be fit accurately with a single doublet.

Following chlorination, GaAs(111)A substrates were immediately exposed to dissolved Grignard reagents in THF. High-resolution XP spectra of chlorinated GaAs(111)A surfaces after reaction with $C_{18}H_{37}MgCl$ in THF are shown in Figure 2.

dx.doi.org/10.1021/la204698a | *Langmuir* 2012, 28, 4672–4682

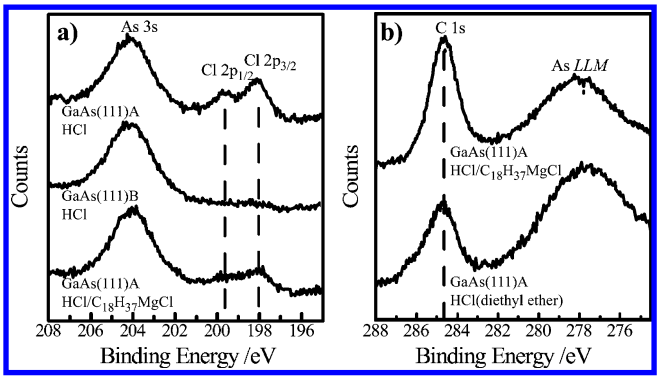

Figure 2. (a) High-resolution XP spectra of Cl 2p region for (top) GaAs(111)A after reaction with HCl in diethyl ether, (middle) GaAs(111)B after reaction with HCl in diethyl ether, and (bottom) GaAs(111)A after sequential reaction first with HCl in diethyl ether and then $C_{18}H_{37}MgCl$ in THF. (b) High-resolution XP C 1s spectra for GaAs(111)A after reaction in (top) HCl in diethyl ether followed by $C_{18}H_{37}MgCl$ in THF and (bottom) HCl in diethyl ether. Spectra are offset for clarity.

Following this sequence, a decrease in surficial Cl from 0.41 ± 0.04 monolayer (ML) to 0.18 ± 0.04 ML was observed. For samples that were not immersed in CH_3OH following exposure to Grignard reagents, detectable levels of Mg, presumably from residual Grignard reagent, were noted. Brief sonication in CH_3OH effectively removed these signatures. Additionally, after reaction with linear chain alkyl Grignard reagents ($C_nH_{2n+1}MgCl$, $n \geq 4$), the measured C 1s intensity was consistently larger than for etched or chlorinated samples. Two separate factors complicated quantitative analysis of the collected C 1s spectra. First, the broad As LLM Auger signal at slightly smaller binding energies than 284 eV masked any possible low-energy shoulder indicative of Ga−C.[50] Second, the presence of adventitious carbon precluded direct determination of surface group content from the intensity of the C 1s signal. Although adventitious carbon was always detected on every measured GaAs surface condition, a pronounced and systematic increase in C 1s signal intensity following exposure to solutions of long alkyl chain Grignard reagents was never observed for GaAs(111)B surfaces. To separately probe the C content of GaAs(111)A surfaces before and after reaction with $C_{18}H_{37}MgCl$, infrared spectra were obtained with a grazing angle attenuated total reflectance accessory (Supporting Information, section S5). After functionalization, the pronounced increase in the intensities of the CH_3- and CH_2- asymmetric and symmetric vibrational modes was consistent with introduction of long alkyl chains to GaAs(111)A specifically via the two-step Grignard reaction sequence (Supporting Information, Figure S6).

To assess the physicochemical properties of GaAs(111)A surfaces following Cl activation and reaction with alkyl Grignard reagents, the wetting properties of reacted surfaces were measured (Table 1). Figure 3 shows the measured sessile drop contact angles between a water droplet and GaAs(111)A surfaces after reaction with several different alkyl Grignard reagents. Freshly etched GaAs(111)A interfaces consistently showed the smallest sessile drop contact angles (45° ± 3°). Etched samples that were then immersed in hot THF without dissolved Grignard reagents showed modestly higher sessile drop contact angle values ("control", 60° ± 4°). Reaction with short alkyl Grignard reagents ($n \leq 2$) did not increase the measured sessile drop contact angle values relative to control samples. Reaction with longer alkyl Grignard reagents ($n \geq 4$)

Table 1. Water Contact Angle Measurements

	water contact angle (deg)		
treatment	GaAs(111)A	GaP(111)A[d]	GaN(0001)
etched[a]	≤20	45 ± 3	36 ± 6
control[b]	≤40	60 ± 4	45 ± 4
$C_{18}H_{37}MgCl$[c]	119 ± 6	107 ± 11	78 ± 3

[a]Degreased and etched to remove native oxide. [b]Same as (a), then Cl-activated, then immersed in hot THF. [c]Same as (a), then Cl-activated, then immersed in THF with Grignard reagent. [d]Data were obtained from ref 34.

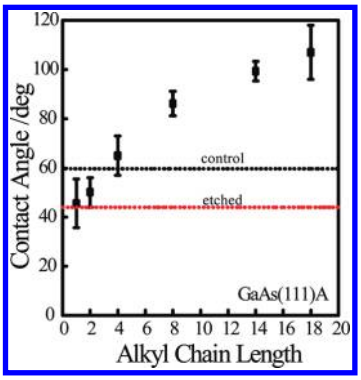

Figure 3. Measured contact angle between sessile water droplet and GaAs(111)A after sequential reaction first with HCl in diethyl ether and then with $C_nH_{2n+2}MgCl$ (n = 1, 2, 4, 8, 14, 18) in THF.

did result in a pronounced increase in hydrophobicity that was larger than the control sample, with longer alkyl Grignard reagents effecting larger sessile drop contact angle values. Measurements for GaAs(111)B interfaces treated in the same manner did not show either a systematic increase in hydrophobicity or values larger than control samples (Supporting Information, Figure S1). These observations support the contention that alkyl groups are selectively attached to GaAs surfaces through a linkage that is specifically favored at the GaAs(111)A face over the GaAs(111)B surface plane.

The amount of residual oxide after reaction with Grignard reagents was determined through high-resolution As 3d XP spectra (Figure 4). Samples that were freshly etched with HCl in diethyl ether consistently showed As 3d spectra indicating no detectable surface oxide. The rates of surface oxidation following surface treatment [either etching for 30 s with concentrated H_2SO_4(aq)[51] or the two-step Grignard reaction sequence] were then measured. GaAs(111)A surfaces etched in H_2SO_4(aq) consistently showed a detectable level of surface oxides inferred from the As 3d spectra (0.23 nm). Prolonged exposure to air resulted in rapid and further oxidation of GaAs(111)A surfaces. After 90 min, both an increase in As_2O_3-type surface oxides and the appearance of spectral features at slightly higher binding energies indicative of As_2O_5-type surface oxides were noted (Figure 4a). In contrast, GaAs(111)A surfaces that had been reacted with $C_{18}H_{37}MgCl$ exhibited a suppressed rate of surface oxidation (Figure 4b). Specifically, after 90 min of exposure to ambient air, the surface oxide content inferred from the As 3d spectra for GaAs(111)A reacted with $C_{18}H_{37}MgCl$ was 8-fold lower than the surface oxide content on etched GaAs(111)A exposed to ambient air for the same period of time (Figure 4c). The GaAs(111)A surfaces were stable in air for prolonged periods, exhibiting less than a monolayer of oxide after 35 days (Supporting Information, Figure S3), but the

dx.doi.org/10.1021/la204698a | Langmuir 2012, 28, 4672−4682

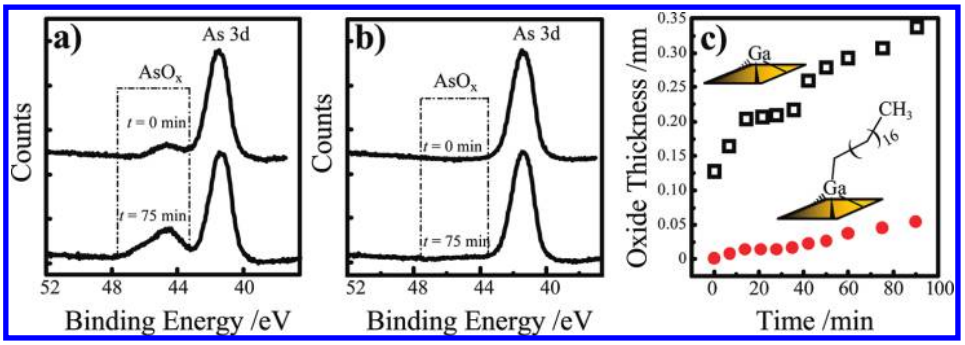

Figure 4. Time-dependent high-resolution As 3d XP spectra for GaAs(111)A surfaces (a) after etching in H_2SO_4(aq) and (b) after sequential reaction first with HCl in diethyl ether and then $C_{18}H_{37}MgCl$ in THF. Spectra are offset for clarity. (c) Measured time-dependent oxide growth from As 3d XP spectra over time for GaAs(111)A surfaces (□) etched in H_2SO_4(aq) and (red circles) after sequential reaction first with HCl in diethyl ether and then with $C_{18}H_{37}MgCl$ in THF.

apparent oxidation rate for these GaAs(111)A surfaces was higher than the oxidation rate for GaP(111)A surfaces treated with the same Grignard reagents.[34] GaAs(111)A surfaces reacted with CH_3MgCl also showed a slightly higher rate of surface oxidation in ambient air (Supporting Information, Figure S2) as compared to similarly treated GaP(111)A surfaces.[34]

High-resolution As 3d XP spectra were also collected to assess the susceptibility of GaAs to chemical attack during immersion in water. GaAs(111)A interfaces were studied that were initially etched in concentrated H_2SO_4(aq) and then immersed in pure water for a total of 27 h. After this period of time, the native surface became visibly roughened, appearing dull and dark brown. High-resolution XP spectra (Figure 5a) showed two important features. First, the intensity of the signature corresponding to oxidized As species exceeded the intensity of the signature for As from the bulk, indicating the surface has become substantially oxidized by water. Second, the overall intensity of the As 3d spectra decreased, as evidenced by the significantly poorer signal-to-noise ratio under the same collection conditions as the data for the initially etched sample. Corresponding survey scans of these two surface types showed that the GaAs(111)A surfaces are Ga-rich; that is, the surfaces become depleted specifically of As (oxidized and reduced) in the near surface region of the samples (Figure 5b). These observations are consistent with the known solubility of oxidized As species in water.[52] In contrast, GaAs(111)A surfaces that were treated with the two-step chlorination−alkylation reaction sequence showed substantial resistance to chemical attack from water. These surfaces remained smooth (mirror polished) even after immersion in water for 27 h, with no visible discoloration. The collected As 3d XP spectra correspondingly showed no appreciable change after 27 h in water (Figure 5c). Specifically, no perceptible increase in signatures indicative of oxidized As species were apparent in the high-resolution As 3d XP spectra, and the As content inferred from the survey scan was the same before and after water immersion (Figure 5d).

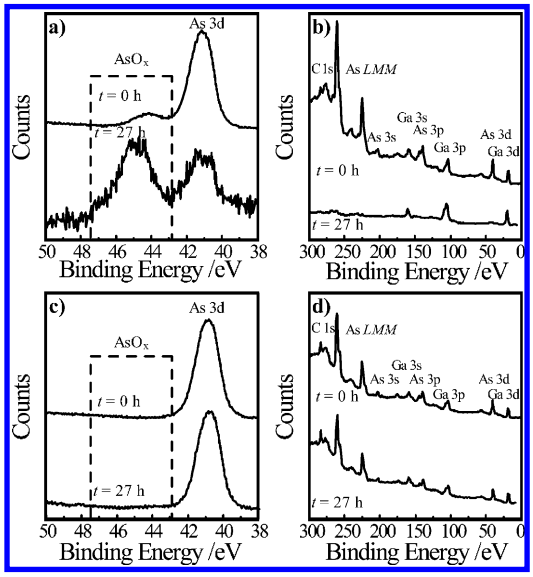

Figure 5. (a, b) XP spectra, (a) high-resolution As 3d and (b) survey, for GaAs(111)A surfaces that were etched in H_2SO_4(aq). The top spectra in panels a and b were obtained immediately after etching, and the bottom spectra were collected after sustained immersion in water for 27 h. (c, d) XP spectra, (c) high-resolution As 3d and (d) survey, for GaAs(111)A surfaces that were sequentially reacted with HCl in diethyl ether solution and then $C_{18}H_{37}MgCl$ in THF. The top spectra in panels c and d were obtained immediately after preparation, and the bottom spectra were collected after sustained immersion in water for 27 h.

Additional experiments were performed to assess the electrical properties of GaAs(111)A surfaces following reaction with Grignard reagents. Figure 6 and Table 2 display the first-order Raman spectral features recorded for GaAs(111)A samples under the spectral acquisition conditions defined above. According to the selection rules for a zincblende crystal structure in the absence of an applied electric field and with optical excitation normal to the (111) surface plane, a pronounced Γ(TO) phonon mode at 268 cm^{-1} is independent of carrier density and the presence/absence of an electric field.[53] Conversely, the Γ(LO) phonon mode at 291 cm^{-1} is strongly sensitive to the magnitude of an electric field, with increased intensity under larger electric fields.[54,55] Specifically, so-called electric-field-induced Raman scattering (EFIRS)[56−59] can be observed at semiconductor surfaces under strong depletion and can be used to gauge the level of band bending and surface defects when (1) the length scale of the depletion layer is on par with the optical probing depth of the Raman experiment and (2) the resultant electric field is large (two conditions satisfied with the experimental conditions employed here). Figure 6a shows that both Γ(TO) and Γ(LO) phonon modes are readily apparent in the spectra for GaAs(111)A surfaces featuring a native oxide. Native oxides at GaAs interfaces possess a high density of electrical defects that trap charge and render a significant potential drop across the near-surface region (i.e., appreciable band bending occurs).[23,53,59] Figure 6 panels b and c depict the presence and

dx.doi.org/10.1021/la204698a | Langmuir 2012, 28, 4672−4682

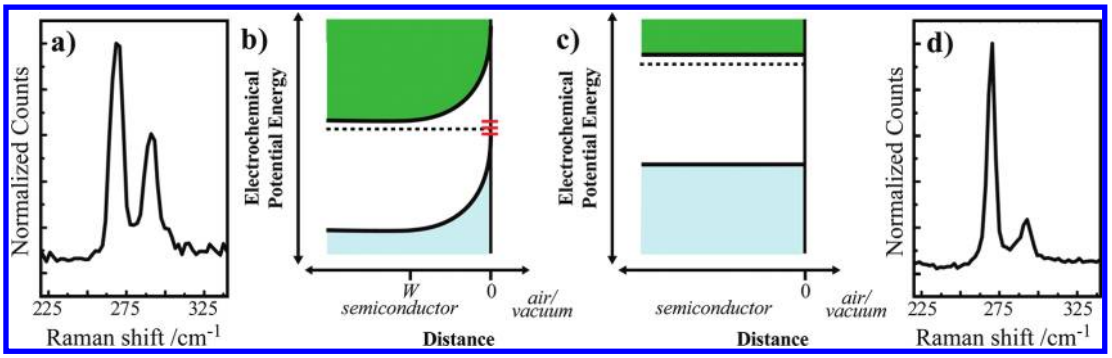

Figure 6. (a) First-order Raman spectrum for GaAs(111)A featuring a native oxide. (b) Idealized depiction of an n-type semiconductor under depletion conditions caused by a high density of surface states. (c) Idealized depiction of the depletion condition of an n-type semiconductor in the absence surface states. (d) First-order Raman spectrum for GaAs(111)A after sequential reaction first with HCl in diethyl ether then $C_{18}H_{37}MgCl$ in THF. Spectra in panels a and d are both normalized to the same *y*-axis scale.

Table 2. Measured Ratio of Phonon Intensity in First-Order Raman Spectra for GaAs(111)A Surfaces

surface treatment	I_{TO}/I_{LO} [a,b]
native oxide	1.98 ± 0.03 (N = 7)
Na_2S (*tert*-butanol)	3.04 ± 0.11 (N = 7)
HCl (diethyl ether)/CH_3MgCl	3.04 ± 0.16 (N = 7)
HCl (diethyl ether)/$C_8H_{17}MgCl$	2.72 ± 0.26 (N = 5)
HCl (diethyl ether)/$C_{14}H_{29}MgCl$	3.68 ± 0.51 (N = 5)
HCl (diethyl ether)/$C_{18}H_{37}MgCl$	2.89 ± 0.08 (N = 5)

[a]Measured ratio of integrated intensities for Γ(TO) and Γ(LO). [b]Errors reported as standard deviation for N sample measurements.

absence of surface depletion for ideal n-type semiconductors featuring a high density and absence of a significant density of surface defects, respectively. Under certain experimental conditions, the logarithm of the integrated intensity of the Γ(LO) mode, I_{LO}, is directly proportional to the product of the depletion layer width, W, in the semiconductor and the absorptivity of the excitation wavelength, $\alpha(\lambda)$.[48,60] In the work shown here, adequate polarization optics on the collection side were not available, and so the contribution to the intensity of the Γ(LO) mode from deformation-potential scattering[53] was not determined, preventing explicit calculation of the magnitude of band bending within each sample. Nevertheless, by using the integrated intensity of the Γ(TO) mode, I_{TO}, as an "internal standard", the ratio I_{TO}/I_{LO} does report on the extent of band bending and, by association, the presence of midgap surface defects that effect depletion conditions. Table 2 shows the values of I_{TO}/I_{LO} for GaAs(111)A substrates coated with a native oxide. Table 2 also shows the value of I_{TO}/I_{LO} recorded for samples treated with 10% Na_2S in *tert*-butanol, a proven (albeit temporary) wet chemical passivation strategy that eliminates surface defects. For comparison, Figure 6d shows a representative Raman spectrum for a GaAs(111)A surface treated with $C_{18}H_{37}MgCl$. In marked contrast to Figure 6a, the intensity of the Γ(LO) phonon mode is substantially suppressed. As indicated by I_{TO}/I_{LO} for alkyl-terminated samples (Table 2), GaAs(111)A samples treated with these Grignard reagents showed responses comparable to those measured for Na_2S(*tert*-butanol)-treated GaAs(111)A surfaces. These data suggest that alkyl-terminated GaAs(111)A surfaces do not possess the same high density of midgap surface trap states that native oxides on GaAs(111)A have. Further, the Raman spectra suggest that the electrical quality of alkyl-terminated GaAs(111)A is comparable to GaAs(111)A surfaces treated with Na_2S(*tert*-butanol), the most effective known wet chemical treatment.[48] A distinct feature of the GaAs(111)A surfaces following reaction with $C_{18}H_{37}MgCl$ is that the Raman signal is stable (Supporting Information, Figure S7). Over the course of 50 min, the measured values of I_{TO}/I_{LO} remained unchanged for GaAs(111)A surfaces treated first with HCl(diethyl ether) and then $C_{18}H_{37}MgCl$. By contrast, the beneficial surface properties induced by immersion in a Na_2S solution are known to be fleeting.[22,48]

A separate probe of the electrical properties of GaAs(111)A surfaces following the two-step chlorination/Grignard reaction sequence was performed through the analysis of Hg/GaAs Schottky heterojunctions.[61] We note that the back contacting scheme described by Nesher et al.[25] yielded heterojunctions whose properties were only partially sensitive to surface changes and so an alternative ohmic contacting approach was used (vide supra). Several types of Hg/GaAs(111)A junctions, including freshly etched GaAs(111)A surfaces, GaAs(111)A surfaces reacted with $C_{18}H_{37}SH$ in ethanol, and GaAs(111)A surfaces reacted with HCl(diethyl ether)/$C_{18}H_{37}MgCl$, were studied. Figure 7a shows representative current density–

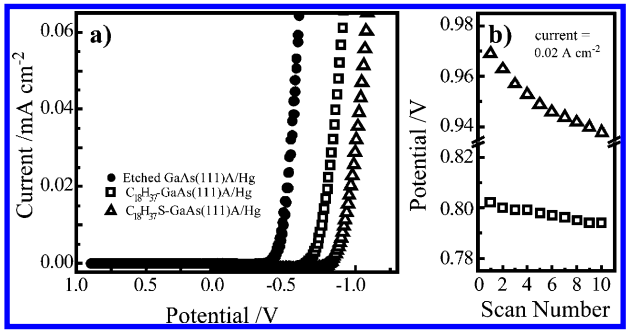

Figure 7. (a) Measured potential-dependent current density for Hg/GaAs heterojunctions featuring (●) GaAs(111)A etched in H_2SO_4(aq), (△) GaAs(111)A functionalized with $C_{18}H_{37}SH$ in ethanol, and (□) GaAs(111)A functionalized with $C_{18}H_{37}MgCl$ in THF. (b) Change in necessary applied bias to drive 0.02 A·cm^{-2} across Hg/GaAs heterojunctions as a function of potential scan number for (△) GaAs(111)A functionalized with $C_{18}H_{37}SH$ in ethanol and (□) GaAs(111)A functionalized with $C_{18}H_{37}MgCl$ in THF.

potential responses for these three types of Hg/GaAs contacts. All three types exhibited strongly rectifying responses, with the etched GaAs(111)A surfaces resulting in the lowest applied bias needed to support a given current density. The Hg/GaAs(111)A heterojunctions featuring surface alkyl chains both

dx.doi.org/10.1021/la204698a | *Langmuir* 2012, 28, 4672–4682

showed more strongly rectifying responses. In principle, both of these heterojunctions feature a similar organic barrier layer between Hg and GaAs consisting of $C_{18}H_{37}$ groups. The observed current density−potential profiles for these two contact types were similar, indicating that both types of long alkyl chain surface groups acted as comparable tunneling barriers that impeded heterogeneous charge transfer between GaAs and Hg. The difference in surface bonds linking the alkyl chains to GaAs (i.e., Ga−C versus Ga−S) apparently was not the defining feature impacting heterogeneous charge transfer in these systems. Figure 7b highlights a secondary difference between these two specific contact types. Figure 7b shows the applied potential required to drive an arbitrary current density of 0.02 A·cm^{-2} across the Hg/GaAs heterojunction. Upon repeated cycling between 0 and 1.2 V, a decrease in the applied potential required to drive this current density was observed for the thiol-modified heterojunctions [(Δpotential)/(Δscan no.) = 3.3 × 10^{-3} V·scan^{-1}]. A possibility for the lowered applied potential needed to supply the desired current could be loss of the thiol surface group and an increasing fraction of direct Hg/GaAs contact area.[25,28] Degradation of $C_{18}H_{37}$S-terminated GaAs(111)A after passage of charge at this current density for 10 scans was confirmed through XP spectra. High-resolution Ga 3d and As 3d spectra both showed GaAs(111)A surfaces with substantial levels of oxide (0.32 nm from As 3d; Supporting Information, Figure S4). For GaAs(111)A surfaces reacted with $C_{18}H_{37}MgCl$, the change in applied bias required to sustain 0.02 A·cm^{-2} after repeated cycling was noticeably smaller [(Δpotential)/(Δscan no.) = 8.7 × 10^{-4} V·scan^{-1}]. Corresponding XP spectra for these surfaces after passage of current showed minimal surface oxidation (0.06 ± 0.01 nm from As 3d; Supporting Information, Figure S5).

GaN. Figure 8 shows a high-resolution XP spectrum for a GaN(0001) film chlorinated with PCl_5 in dichlorobenzene.

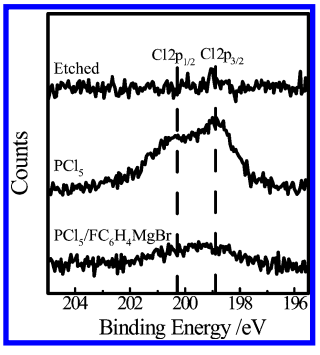

Figure 8. High-resolution Cl 2p XP spectra for GaN(0001) surfaces, (top) after etching in KOH(aq), (middle) after reaction with PCl_5 in chlorobenzene, and (bottom) after sequential reaction first with PCl_5 in chlorobenzene and then C_6H_4FMgBr in THF. Spectra are offset for clarity.

In contrast to GaAs but similar to GaP,[34] this wet chemical chlorination scheme did not induce macroscopic surface pitting of GaN(0001), in accord with the previously recognized chemical inertness of GaN toward corrosive environments.[62−64] Reaction of GaN(0001) with PCl_5 in dichlorobenzene did effect a slight increase in the measured surface topography, as indicated through atomic force microscopy (Supporting Information, Figure S10). Corresponding Cl 2p XP spectra showed the presence of surficial Cl higher than attainable with HCl in diethyl ether (1.2 ± 0.2 versus 0.6 ± 0.2 ML, respectively). For this reason, PCl_5 was used for reactions with Grignard reagents in THF as described above. After reaction with $C_{18}H_{37}MgCl$, GaN(0001) films became noticeably more hydrophobic. Sessile drop contact angles with water increased relative to either the etched or control treatments (Table 1). The measured value of 78° ± 3° for GaN(0001) reacted with $C_{18}H_{37}MgCl$ was consistent with a surface featuring hydrophobic groups but was less than the corresponding value for similarly treated GaAs(111)A and GaP(111)A[34] wetting contact angles.

XP spectra of GaN(0001) surfaces following exposure to Grignard reagents were collected. Even though there were no overlapping Auger signals near 284 eV for GaN samples, analyses of the C 1s XP spectra were still complicated. Conclusive determination of Ga−C surface bonds was problematic since GaN(0001) samples produced through chemical vapor deposition (CVD) from organogallium precursors natively show a detectable and inhomogeneous content of residual Ga−C-containing species within the probing volume of our X-ray photoelectron spectrometer. Specifically, Ga-bound carbon impurities in CVD-based GaN films show a spectroscopic feature that mimics the low binding energy shoulder ascribed to surficial Ga−C bonding.[34] For this reason, commercial GaN films without residual organic contaminants were employed. For these samples, no signatures at binding energies more positive than 284 eV were observed in the C 1s spectra for etched or control experiments. However, the high-resolution C 1s spectra for GaN(0001) samples that were first reacted with PCl_5 and then CH_3MgCl did show a shoulder at 282.7 eV (Figure 9). The integrated intensity of this spectral feature

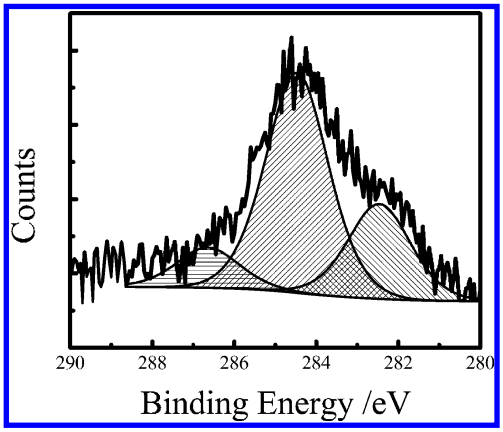

Figure 9. High-resolution C 1s XP spectrum for GaN(0001) after sequential reaction with PCl_5 in chlorobenzene and then CH_3MgCl in THF.

corresponded to a CH_3 surface coverage of 0.47 ± 0.02 ML, less than previously observed for similarly treated GaP(111)A.[34] High-resolution F 1s spectra for GaN(0001) surfaces were also obtained following etching, chlorination, and reaction with C_6H_4FMgBr to determine whether surface functionalization occurred at GaN(0001) surfaces under the employed conditions (Figure 10). As seen with GaAs(111)A surfaces, the apparent carbon content (as indicated by the C 1s signal intensity) increased significantly after exposure to Grignard reagent. Concomitantly, the measured Cl 2p intensities were significantly attenuated (Figure 8). The remaining Cl signature after reaction with Grignard reagent could still be fit with the same doublet, although the low signal intensity made it difficult to analyze these data. This trend was observed consistently for both this aryl

dx.doi.org/10.1021/la204698a | Langmuir 2012, 28, 4672−4682

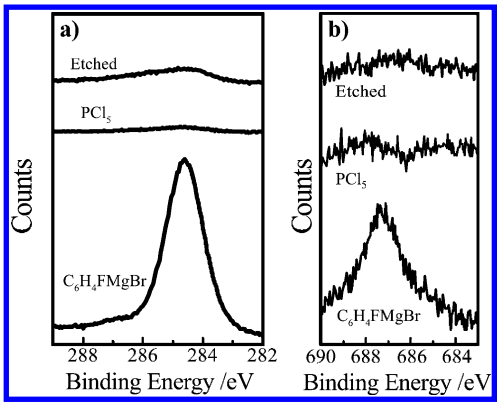

Figure 10. High-resolution (a) C 1s and (b) F 1s XP spectra for GaN(0001) surfaces (top) after etching in 1 M KOH(aq), (middle) after reaction with PCl_5 in chlorobenzene, and (bottom) after sequential reaction first with PCl_5 in chlorobenzene and then with C_6H_4FMgBr in THF.

Grignard reagent and linear chain alkyl Grignard reagents, although the total C 1s intensity varied somewhat due to the residual adventitious carbon content. High-resolution F 1s spectra are shown in Figure 10b. Fluorine is not present in either adventitious carbon or carbon contaminant from film deposition. Therefore, detection of F signatures is a direct indicator that the Grignard reaction sequence results in C_6H_4FMgBr groups attached to the surface. Figure 10b shows that a detectable F 1s singlet was obtained only after exposure to C_6H_4FMgBr, consistent with the premise that this reaction sequence produces covalently grafted C_6H_4F groups onto GaN(0001) surfaces. The magnitude of the F 1s signal was invariant toward repeated washing/sonication in neat methanol, indicating the signal did not arise purely from physisorbed and unreacted reagents. Makowski et al.[13] have also recently shown the functionalization of GaN surfaces with organic groups. However, the surface functionalization approach in that work required the use of an initial H_2 plasma activation step, and C 1s spectroscopic evidence of a Ga−C surface bond was not shown. The data shown here represent organic groups grafted to unoxidized GaN(0001) interfaces by purely wet chemical treatments.

DISCUSSION

The cumulative results from this report on GaAs and GaN interfaces, in conjunction with our earlier study of GaP surfaces, indicate that the atop Ga atoms at the surfaces of binary III−V semiconductors are reactive toward alkylation reagents. The net process mirrors both the classic, homogeneous inorganic synthesis of organogallium compounds from $GaCl_3$ and alkyl Grignard reagents[65−67] and the more recently studied heterogeneous Si and Ge surface Grignard reaction chemistry.[7,68−72] Hence, the data shown here for atop Ga atoms at the GaAs(111)A, GaP(111)A, and GaN(0001) surface planes, in conjunction with relatively low reaction yields observed with the GaAs(111)B and GaP(111)B surface planes, support the contention that organic groups can be grafted specifically through surface Ga−C bonds.

The demonstration of wet chemical strategies that covalently link functional groups to nonoxidized Ga-containing III−V semiconductor interfaces has both applied and fundamental implications. Surface modification strategies utilizing oxidized surfaces (e.g., silanization, phosphonate chemisorption)[73−76] are problematic for GaAs, GaP, and GaN surfaces in many optoelectronic applications. Oxidized Ga-based III−V semiconductor interfaces unavoidably contain large quantities of electronic surface traps (i.e., $\geq 10^{13}$ defects·cm^{-2}).[77,78] For example, in the context of solar energy conversion applications, surface-mediated charge recombination at interfacial defects is a deleterious, parasitic pathway.[79] Modification schemes based on oxidized surfaces are wholly inappropriate and incompatible. The analysis of Schottky junctions performed here indicate that the wet chemical chlorination−Grignard reaction sequence produces GaAs heterojunctions with stability toward the passage of current, in contrast to other wet chemical strategies.[10] Surface groups coordinated through σ-bonds are believed to be particularly effective for electronic passivation.[23,80] The presented Raman data strongly support the notion that a GaAs(111)A interface featuring a layer of alkyl groups introduced via Grignard reaction chemistry constitutes a surface with a much lower density of midgap electrical traps than a GaAs(111)A surface with a native oxide. Separate time-resolved photoluminescence or photoconductivity measurements,[23,29,30,81,82] performed with high quality (i.e., long bulk lifetime) GaAs materials, would be useful to determine the specific level of midgap surface defects and trap-based recombination before and after the two-step chlorination/Grignard reaction sequence. The Raman spectra shown here should serve as impetus for such work. Nevertheless, the measured I_{TO}/I_{LO} values shown here strongly suggest that the presence of alkyl chains results in GaAs surface electronic properties comparable to GaAs interfaces following wet chemical sulfide treatments. This feature is in contrast to other wet chemical routes that functionalize surfaces without passivating surface defects.[9,10,22] Since the prevailing thought in GaAs surface science is that surface traps at the native surface are As-based in nature,[23] the observation that surface reactions directed toward bonding at atop Ga lowers surface defect density may be surprising. However, the data shown here are consistent with the premise that coordination of surficial Ga indirectly imparts stability on surface As atoms, limiting (or severely slowing) the extent of As-based surface reactions. This observation may prove useful since surface As species are notoriously reactive.[23] For GaN (and GaP), the extent that surface alkylation through putative Ga−C bonds lowers surface defect density remains undefined.

An important conclusion from the present studies is that surface alkylation improves surface stability with respect to oxidation. The XP spectra shown here and previously[34] demonstrate that GaAs and GaP interfaces featuring alkyl groups are markedly less susceptible to undesirable surface oxidation under ambient conditions. The observed chemical stability likely arises from a high density of surface groups that sterically impede surface attack. The measured contact angles with water droplets for GaAs (111)A and GaP(111)A surfaces following reaction with $C_{18}H_{37}MgCl$ suggests that the introduced surface layer is more dense than on GaN(0001) after reaction with $C_{18}H_{37}MgCl$.[20,83,84] These observations are in accord with the distances between adjacent Ga atop atoms at GaAs(111)A and GaP(111)A surfaces (0.399 and 0.385 nm, respectively),[85,86] which are better matched to the areal footprint of a linear alkane chain than the 0.319 nm surface atom spacing at GaN(0001). However, for GaN, a lower density of surface groups may not be as critical since GaN surfaces are more naturally resistant to chemical attack.[87,88]

Reactions between nucleophilic reagents and electrophilic Ga atoms that produce stable bonds have precedent in homogeneous and heterogeneous reaction chemistries. Although

dx.doi.org/10.1021/la204698a | Langmuir 2012, 28, 4672−4682

simple organogallium compounds like $Ga(CH_3)_3$ are typically not stable in air or moisture, exceedingly stable Ga−C bonds have been achieved in N-heterocyclic carbene−$GaCl_3$ adducts. These compounds show indefinite stability in air and in solution[89] and feature a four-coordinate Ga atom bound by a strong σ-donor ligand. It is presently unclear whether the putative surficial Ga−C bonds effected through the reaction of III−V semiconductors and Grignard reagents more closely resemble the bonding in these adducts or in simple compounds like $Ga(CH_3)_3$. The data suggest the former. To be clear, the stability indicated by the data in this work exceeds that achieved with other nucleophilic reagents like PCl_3 and N_2H_4.[12,14,90,91] In addition to stability in ambient and wet conditions, an advantage of surface passivation layers from Grignard reagents over passivation reagents like PCl_3 and N_2H_4 is the possibility of secondary surface functionalization when partially unsaturated organic surface groups are introduced.[92] Although versatile and attractive for practical reasons, Grignard reagents are neither the only nor the most nucleophilic reagents for alkylation. For example, organolithium and organozinc reagents tend to show greater and weaker nucleophilicity, respectively.[37,66] Surface alkylation through nucleophilic attack may be a general wet chemical reaction pathway for III−V surfaces, and additional types of alkylation reagents should be explored. Regarding Grignard reagents, the principal mechanism by which surface reaction occurs is not clear. None of the presented experiments provides direct insight on whether the surface bonding formation is mechanistically related to either homogeneous organogallium reactions or heterogeneous group IV semiconductor passivation. Since Ga−Cl bond exchange for putative Ga−C surface bonds should be sensitive to surface site spacing and the covalent character of Ga−V bonds, the differences in wettability and stability across GaN(0001), GaP(111)A, and GaAs(111)A surfaces noted in this work are not surprising. Still, the premise that Cl termination provides a consistent, reproducible, and metastable surface reactive condition appears valid for GaAs, GaN, and GaP. Studies that explore whether the extent of surface coverage and/or resultant surface properties is affected noticeably by the nucleophilic character of the alkylation reagent and or halide termination step would be useful. To date, few experiments have been performed that directly probe the wet chemical reactivity of a family of related semiconductor surfaces toward σ-bonding reagents. In this regard, the data shown here complete a report on the wet chemical reactivity between an alkylating reagent and a family of related III−V semiconductor surfaces.

SUMMARY

Crystalline gallium arsenide (GaAs) and gallium nitride (GaN) surfaces have been functionalized with alkyl groups via a sequential wet chemical Cl activation−Grignard reaction process. These results, in conjunction with previous studies on GaP, show that atop Ga atoms on structurally related Ga-based binary III−V semiconductors can be deliberately functionalized with putative Ga−C surface bonds. For GaAs, the collected Raman spectra specifically indicate a lowering of deleterious electrical surface defects at a level comparable to the existing state-of-the-art in chemical passivation techniques. For GaN, the cumulative data illustrate a purely wet chemical method for modifying interfacial characteristics. Overall, these results highlight the largely unexplored possibilities of using nucleophilic alkylation reagents for modifying, improving, and controlling the physicochemical and electrochemical properties of both GaAs and GaN.

ASSOCIATED CONTENT

Supporting Information

Additional text and 10 figures, showing water contact angle measurements for GaAs(111)B; XP spectra of functionalized GaAs(111)A after exposure to air, water, and passage of current; IR spectra of a GaAs(111)A surface following reaction with $C_{18}H_{37}MgCl$; time-dependent Raman measurements; XP spectra of chemically treated GaN(0001) surfaces; and AFM images of GaN(0001) surfaces before and after chlorination treatment. This material is available free of charge via the Internet at http://pubs.acs.org/.

AUTHOR INFORMATION

Corresponding Author

*Phone 734-647-4750; e-mail smald@umich.edu.

Notes

The authors declare no competing financial interest.

ACKNOWLEDGMENTS

We thank Professor P. C. Ku for providing initial GaN substrates for analysis. We also thank the University of Michigan in support of this work.

REFERENCES

(1) Bent, S. F. *Surf. Sci.* **2002**, *500*, 879−903.
(2) Filler, M. A.; Bent, S. F. *Prog. Surf. Sci.* **2003**, *73*, 1−56.
(3) Linford, M. R.; Fenter, P.; Eisenberger, P. M.; Chidsey, C. E. D. *J. Am. Chem. Soc.* **1995**, *117*, 3145−3155.
(4) Buriak, J. M. *Chem Commun* **1999**, 1051−1060.
(5) Buriak, J. M. *Chem. Rev.* **2002**, *102*, 1271−1308.
(6) Hamers, R. J. *Annu. Rev. Anal. Chem.* **2008**, *1*, 707−736.
(7) Gerlich, D.; Cullen, G. W.; Amick, J. A. *J. Electrochem. Soc.* **1962**, *109*, 133−138.
(8) Hamers, R. J.; Coulter, S. K.; Ellison, M. D.; Hovis, J. S.; Padowitz, D. F.; Schwartz, M. P.; Greenlief, C. M.; Russell, J. N. *Acc. Chem. Res.* **2000**, *33*, 617−624.
(9) Cohen, R.; Kronik, L.; Shanzer, A.; Cahen, D.; Liu, A.; Rosenwaks, Y.; Lorenz, J. K.; Ellis, A. B. *J. Am. Chem. Soc.* **1999**, *121*, 10545−10553.
(10) Stewart, M. P.; Maya, F.; Kosynkin, D. V.; Dirk, S. M.; Stapleton, J. J.; McGuiness, C. L.; Allara, D. L.; Tour, J. M. *J. Am. Chem. Soc.* **2004**, *126*, 370−378.
(11) Seker, F.; Meeker, K.; Kuech, T. F.; Ellis, A. B. *Chem. Rev.* **2000**, *100*, 2505−2536.
(12) Berkovits, V. L.; Ulin, V. P.; Losurdo, M.; Capezzuto, P.; Bruno, G.; Perna, G.; Capozzi, V. *Appl. Phys. Lett.* **2002**, *80*, 3739−3741.
(13) Makowski, M. S.; Zemlyanov, D. Y.; Ivanisevic, A. *Appl. Surf. Sci.* **2011**, *257*, 4625−4632.
(14) Traub, M. C.; Biteen, J. S.; Michalak, D. J.; Webb, L. J.; Brunschwig, B. S.; Lewis, N. S. *J. Phys. Chem. C* **2008**, *112*, 18467−18473.
(15) Adlkofer, K.; Tanaka, M. *Langmuir* **2001**, *17*, 4267−4273.
(16) Jun, Y.; Zhu, X. Y.; Hsu, J. W. P. *Langmuir* **2006**, *22*, 3627−3632.
(17) Baum, T.; Ye, S.; Uosaki, K. *Langmuir* **1999**, *15*, 8577−8579.
(18) Shaporenko, A.; Adlkofer, K.; Johansson, L. S. O.; Tanaka, M.; Zharnikov, M. *Langmuir* **2003**, *19*, 4992−4998.
(19) Shaporenko, A.; Adlkofer, K.; Johansson, L. S. O.; Ulman, A.; Grunze, M.; Tanaka, M.; Zharnikov, M. *J. Phys. Chem. B* **2004**, *108*, 17964−17972.
(20) McGuiness, C. L.; Blasini, D.; Masejewski, J. P.; Uppili, S.; Cabarcos, O. M.; Smilgies, D.; Allara, D. L. *ACS Nano* **2007**, *1*, 30−49.
(21) Sheen, C. W.; Shi, J.-X.; Mirtensson, J.; Parikh, A. N.; Allara, D. L. *J. Am. Chem. Soc.* **1992**, *114*, 1514−1515.
(22) McGuiness, C. L.; Shaporenko, A.; Zharnikov, M.; Walker, A. V.; Allara, D. L. *J. Phys. Chem. C* **2007**, *111*, 4226−4234.

(23) Lunt, S. R.; Ryba, G. N.; Santangelo, P. G.; Lewis, N. S. *J. Appl. Phys.* **1991**, *70*, 7449−7465.
(24) Ashkenasy, G.; Cahen, D.; Cohen, R.; Shanzer, A.; Vilan, A. *Acc. Chem. Res.* **2002**, *35*, 121−128.
(25) Nesher, G.; Shpaisman, H.; Cahen, D. *J. Am. Chem. Soc.* **2007**, *129*, 734−735.
(26) Salomon, A.; Bolcking, T.; Gooding, J. J.; Cahen, D. *Nano Lett.* **2006**, *6*, 2873−2876.
(27) Vilan, A.; Shanzer, A.; Cahen, D. *Nature* **2000**, *404*, 166−168.
(28) Nesher, G.; Vilan, A.; Cohen, H.; Cahen, D.; Amy, F.; Chan, C.; Hwang, J.; Kahn, A. *J. Phys. Chem. B* **2006**, *110*, 14363−14371.
(29) Yablonovitch, E.; Bhat, R.; Harbison, J. P.; Logan, R. A. *Appl. Phys. Lett.* **1987**, *50*, 1197−1199.
(30) Yablonovitch, E.; Gmitter, T. J. *Solid-State Electron.* **1992**, *35*, 261−267.
(31) Tomioka, K.; Motohisa, J.; Hara, S.; Hiruma, K.; Fukui, T. *Nano Lett.* **2010**, *10*, 1639−1644.
(32) Vetury, R.; Zhang, N. Q.; Keller, S.; Mishra, U. K. *IEEE Trans. Electron Devices* **2001**, *48*, 560−566.
(33) Gila, B. P.; Thaler, G. T.; Onstine, A. H.; Hlad, M.; Gerger, A.; Herrero, A.; Allums, K. K.; Stodilka, D.; Jang, S.; Kang, B.; Anderson, T.; Abernathy, C. R.; Ren, F.; Pearton, S. J. *Solid-State Electron.* **2006**, *50*, 1016−1023.
(34) Mukherjee, J.; Peczonczyk, S.; Maldonado, S. *Langmuir* **2010**, *26*, 10890−10896.
(35) Mao, O.; Altounian, Z.; StromOlsen, J. O. *Rev. Sci. Instrum.* **1997**, *68*, 2438−2441.
(36) Shriver, D. F.; Drezdzon, M. A. *The Manipulation of Air-Sensitive Compounds*; Wiley: New York, 1986.
(37) Bansal, A.; Li, X.; Yi, S. I.; Weinberg, W. H.; Lewis, N. S. *J. Phys. Chem. B* **2001**, *105*, 10266−10277.
(38) Wagner, C. D.; Riggs, W. M.; Davis, L. E.; Moulder, J. F.; Muilenberg, G. E. *Handbook of X-Ray Photoelectron Spectroscopy*; Perkin Elmer Corporation: Eden Prairie, MN, 1979.
(39) Traub, M. C.; Biteen, J. S.; Michalak, D. J.; Webb, L. J.; Brunschwig, B. S.; Lewis, N. S. *J. Phys. Chem. B* **2006**, *110*, 15641−15644.
(40) *Practical Surface Analysis by Auger and X-Ray Photoelectron Spectroscopy*; Briggs, D., Seah, M. P., Eds.; John Wiley & Sons: New York, 1984.
(41) Butcher, D. N.; Sealy, B. J. *Electron. Lett.* **1977**, *13*, 558−559.
(42) Wasilewski, Z. R.; Baribeau, J.-M.; Beaulieu, M.; Wu, X.; Sproule, G. I. *J. Vac. Sci. Technol. B: Microelectron. Nanometer Struct.—Process., Meas., Phenom.* **2004**, *22*, 1534−1538.
(43) Chibowski, E.; Terpilowski, K. *J. Colloid Interface Sci.* **2008**, *319*, 505−513.
(44) Tadmor, R. *Langmuir* **2004**, *20*, 7659−7664.
(45) Aspnes, D. E.; Studna, A. A. *Phys. Rev. B* **1983**, *27*, 985−1009.
(46) Bessolov, V. N.; Lebedev, M. V. *Semiconductors* **1998**, *32*, 1141−1156.
(47) Bessolov, V. N.; Lebedev, M. V.; Ivankov, A. F.; Bauhofer, W.; Zahn, D. R. T. *Appl. Surf. Sci.* **1998**, *133*, 17−22.
(48) Bessolov, V. N.; Lebedev, M. V.; Zahn, D. R. T. *J. Appl. Phys.* **1997**, *82*, 2640−2642.
(49) Lu, Z. H.; Lagarde, C.; Sacher, E.; Currie, J. F.; Yelon, A. *J. Vac. Sci. Technol. A* **1988**, *7*, 646−650.
(50) Jun, Y.; Zhu, X.-Y.; Hsu, J. W. P. *Langmuir* **2006**, *22*, 3627−3632.
(51) Yao, H.; Yau, S. L.; Itaya, K. *Appl. Phys. Lett.* **1996**, *68*, 1473−1475.
(52) Aspnes, D. E.; Studna, A. A. *Appl. Phys. Lett.* **1985**, *46*, 1071−1073.
(53) Geurts, J. *Surf. Sci. Rep.* **1993**, *18*, 1−89.
(54) Nakamura, T.; Katoda, T. *J. Appl. Phys.* **1984**, *55*, 3064−3067.
(55) Olego, D. J.; Schachter, R.; Baumann, J. *J. Vac. Sci. Technol., B: Microelectron. Nanometer Struct.—Process., Meas., Phenom.* **1985**, *3*, 1097−1098.
(56) Fleury, P. A.; Worlock, J. M. *Phys. Rev. Lett.* **1967**, *18*, 665−667.
(57) Pinczuk, A.; Burstein, E. *Phys. Rev. Lett.* **1968**, *21*, 1073−1075.
(58) Scott, J. F.; Fleury, P. A.; Worlock, J. M. *Phys. Rev.* **1969**, *177*, 1288−1291.
(59) Cape, J. A.; Tennant, W. E.; Hale, L. G. *J. Vac. Sci. Technol.* **1977**, *14*, 921−923.
(60) Chen, X.; Si, X.; Malhotra, V. *J. Electrochem. Soc.* **1993**, *140*, 2085−2088.
(61) Maldonado, S.; Plass, K. E.; Knapp, D.; Lewis, N. S. *J. Phys. Chem. C* **2007**, *111*, 17690−17699.
(62) Zhuang, D.; Edgar, J. H. *Mater. Sci. Eng., R* **2005**, *48*, 1−46.
(63) King, S. W.; Barnak, J. P.; Bremser, M. D.; Tracy, K. M.; Ronning, C.; Davis, R. F.; Nemanich, R. J. *J. Appl. Phys.* **1998**, *84*, 5248−5260.
(64) Basak, D.; Verdu, M.; Montojo, M. T.; SanchezGarcia, M. A.; Sanchez, F. J.; Munoz, E.; Calleja, E. *Semicond. Sci. Technol.* **1997**, *12*, 1654−1657.
(65) Andrews, P. C.; Junk, P. C.; Nuzhnaya, I.; Spiccia, L.; Vanderhoek, N. *J. Organomet. Chem.* **2006**, *691*, 3426−3433.
(66) Robinson, G. H. In *Encyclopedia of Inorganic Chemistry*; John Wiley & Sons, Ltd: New York, 2006.
(67) Jones, A. C.; Holliday, A. K.; Colehamilton, D. J.; Ahmad, M. M.; Gerrard, N. D. *J. Cryst. Growth* **1984**, *68*, 1−9.
(68) Rivillon, S.; Michalak, D. J.; Chabal, Y. J.; Wielunski, L.; Hurley, P. T.; Lewis, N. S. *J. Phys. Chem. C* **2007**, *111*, 13053−13061.
(69) Bansal, A.; Li, X. L.; Lauermann, I.; Lewis, N. S.; Yi, S. I.; Weinberg, W. H. *J. Am. Chem. Soc.* **1996**, *118*, 7225−7226.
(70) Fellah, S.; Boukherroub, R.; Ozanam, F.; Chazalviel, J. N. *Langmuir* **2004**, *20*, 6359−6364.
(71) Fellah, S.; Teyssot, A.; Ozanam, F.; Chazalviel, J. N.; Vigneron, J.; Etcheberry, A. *Langmuir* **2002**, *18*, 5851−5860.
(72) Vegunta, S. S.; Ngunjiri, J. N.; Flake, J. C. *Langmuir* **2009**, *25*, 12750−12756.
(73) Kim, H.; Colavita, P. E.; Paoprasert, P.; Gopalan, P.; Kuech, T. F.; Hamers, R. J. *Surf. Sci.* **2008**, *602*, 2382−2388.
(74) Bolts, J. M.; Wrighton, M. S. *J. Am. Chem. Soc.* **1979**, *101*, 6179−6184.
(75) Kang, B. S.; Ren, F.; Wang, L.; Lofton, C.; Weihong, W. T.; Pearton, S. J.; Dabiran, A.; Osinsky, A.; Chow, P. P. *Appl. Phys. Lett.* **2005**, *87*, No. 023508.
(76) Baur, B.; Steinhoff, G.; Hernando, J.; Purrucker, O.; Tanaka, M.; Nickel, B.; Stutzmann, M.; Eickhoff, M. *Appl. Phys. Lett.* **2005**, *87*, No. 263901.
(77) Ahrenkiel, R. K.; Dunlavy, D. J. *Solid-State Electron.* **1984**, *27*, 485−489.
(78) Faraz, S. M.; Ashraf, H.; Arshad, M. I.; Hageman, P. R.; Asghar, M.; Wahab, Q. *Semicond. Sci. Technol.* **2010**, 25.
(79) Fonash, S. *Solar Cell Device Physics*, 2nd ed.; Academic Press: Burlington, MA, 2010.
(80) Bent, S. F. *ACS Nano* **2007**, *1*, 10−12.
(81) Dmitruk, N. L.; Lyashenko, V. I.; Tereshenko, A. K.; Spektor, S. A. *Phys. Status Solidi A* **1973**, *20*, 53−62.
(82) Hovel, H. J.; Guidotti, D. *IEEE Trans. Electron Devices* **1985**, *32*, 2331−2338.
(83) Rosu, D. M.; Jones, J. C.; Hsu, J. W. P.; Kavanagh, K. L.; Tsankov, D.; Schade, U.; Esser, N.; Hinrichs, K. *Langmuir* **2009**, *25*, 919−923.
(84) Rodriguez, L. M.; Gayone, J. E.; Sanchez, E. A.; Grizzi, O.; Blum, B.; Salvarezza, R. C.; Xi, L.; Lau, W. M. *J. Am. Chem. Soc.* **2007**, *129*, 7807−7813.
(85) Smart, L. E.; Moore, E. A. *Solid State Chemistry: an Introduction*, 3rd ed.; Taylor & Francis Group: New York, 2005.
(86) Massa, W. *Crystal Structure Determination*; 2nd ed.; Springer: New York, 2002.
(87) Mileham, J. R.; Pearton, S. J.; Abernathy, C. R.; MacKenzie, J. D.; Shul, R. J.; Kilcoyne, S. P. *J. Vac. Sci. Technol. A* **1996**, *14*, 836−839.
(88) Minsky, M. S.; White, M.; Lu, E. L. *Appl. Phys. Lett.* **1996**, *68*, 1531−1533.

(89) Marion, N.; Escudero-Adan, E. C.; Benet-Buchholz, J.; Stevens, E. D.; Fensterbank, L.; Malacria, M.; Nolan, S. P. *Organometallics* **2007**, *26*, 3256−3259.
(90) Singh, N. K.; Doran, D. C. *Surf. Sci.* **1999**, *422*, 50−64.
(91) Kropewnicki, T. J.; Kohl, P. A. *J. Vac. Sci. Technol. A* **1998**, *16*, 139−144.
(92) Plass, K. E.; Liu, X.; Brunschwig, B. S.; Lewis, N. S. *Chem. Mater.* **2008**, *20*, 2228−2233.